A Combined Timing and Frequency Synchronization and Channel Estimation for OFDM

Hlaing Minn,[*]*Member, IEEE*, Vijay K. Bhargava,[†]*Fellow, IEEE*, and Khaled Ben Letaief,[‡]*Fellow, IEEE*
[*] Electrical Engineering Dept., University of Texas at Dallas, TX 75083-0688. (hlaing.minn@utdallas.edu)
[†] Electrical & Computer Engineering Dept., University of British Columbia, Canada. (vijayb@ece.ubc.ca)
[‡] Electrical & Electronic Engineering Dept., Hong Kong University of Science & Technology (eekhaled@ee.ust.hk)

***Abstract*— The idea of combined timing and frequency synchronization and channel estimation is quite desirable since the synchronization and channel estimation tasks can affect each other. This paper addresses training signal based combined timing and frequency synchronization and channel estimation for OFDM systems. The proposed scheme consists of two stages. At the first stage, coarse timing and frequency offset estimates are obtained. Based on these estimates, a (coarse) channel response estimate is obtained. The timing and frequency offset estimates at the second stage are obtained by a maximum likelihood (ML) realization based on sliding observation vector. Then a ML channel estimation is performed. The simulation results show that the proposed combined approach performs quite well and circumvents the problem of mismatch among individual synchronization tasks.**

I. Introduction

OFDM systems are much more sensitive to synchronization errors than single carrier systems. Several approaches have been proposed for timing synchronization (e.g. [1]-[2]) and frequency synchronization (e.g. [3]-[4]), separately. These separate frequency synchronization methods assume perfect timing synchronization, which may not be guaranteed, and timing estimation errors may affect frequency synchronization. In order to evaluate actual performance, joint timing and frequency synchronization approaches (e.g., [5]-[6]) are desirable. Coherent OFDM systems require channel estimation. Previous work on OFDM channel estimation (e.g. [8]-[9]) assume perfect synchronization. However, this may not be guaranteed and synchronization errors can deteriorate the channel estimation performance [10]. Hence, a desirable approach which reflects a more accurate performance is to address synchronization and channel estimation tasks together.

In this paper, we consider a combined approach for estimation of timing offset, frequency offset, and channel for an OFDM system using a training signal. The joint estimation of timing offset, frequency offset and channel impulse response is broken down into two stages. At the first stage, coarse timing offset estimation and coarse frequency offset estimation are performed. At the second stage, the ML realization of the fine joint timing and frequency offset estimation is performed based on the sliding observation vector (SOV) and using the coarse sync parameters. Then an ML-based channel estimation is performed. The simulation results show that the proposed combined approach performs quite well and circumvents the problem of mismatch among individual synchronization tasks.

II. Signal Model

The complex baseband samples of an OFDM symbol, at the sampling rate $1/T$ (N times sub-carrier spacing), are given by

$$s(k) = \frac{1}{\sqrt{N}} \sum_{n=0}^{N-1} c_n \; exp(j2\pi kn/N), \;\; -N_g \le k \le N-1 \quad (1)$$

where c_n is modulated data (zeros for null sub-carriers), N is the number of IFFT points, N_g is the number of cyclic prefix (CP) samples and $j = \sqrt{-1}$. Consider a frequency selective multipath fading channel characterized by the sample-spaced channel impulse response (CIR)

$$h(k) = exp(j\phi) \sum_{l} h_l \; p(kT - \tau_l - t_0), \; k = 0, \, 1, \, \ldots, \, K-1 \quad (2)$$

where $p(t)$ is the combined response of transmit and receive filters, t_0 is a delay to make the filter response causal, $\{h_l\}$ are complex path gains of the channel, $\{\tau_l\}$ are the path delays, ϕ is an arbitrary carrier phase and K is the effective maximum channel delay spread in samples. Assuming perfect sampling clock and no oscillator phase noise, the received sample can be given by

$$r(k) = exp(j2\pi kv/N) \sum_{l=0}^{K-1} h(l) s(k-l) + n(k) \quad (3)$$

where v is the carrier frequency offset normalized by the sub-carrier spacing, $\{n(k)\}$ are independent and identically distributed, zero-mean complex Gaussian noise samples with variance σ_n^2, $-N_g + K - 1 \le k \le N-1$ and $N_g > K$.

Define the following for a training symbol with N_g samples of CP part and $(\beta+1)$ samples of the useful part:

$$\begin{aligned}
\boldsymbol{r}_\gamma(\varepsilon) &\triangleq [r(\varepsilon-\gamma) \; r(\varepsilon-\gamma+1) \; \ldots \; r(\varepsilon+\beta)]^T \\
\boldsymbol{h} &\triangleq [h(0) \; h(1) \; \ldots \; h(K-1)]^T \\
\boldsymbol{W}_\gamma(v,\varepsilon) &\triangleq diag\{e^{\frac{j2\pi(\varepsilon-\gamma)v}{N}}, e^{\frac{j2\pi(\varepsilon-\gamma+1)v}{N}}, \; \ldots, \; e^{\frac{j2\pi(\varepsilon+\beta)v}{N}}\} \\
\boldsymbol{n}_\gamma(\varepsilon) &\triangleq [n(\varepsilon-\gamma) \; n(\varepsilon-\gamma+1) \; \ldots \; n(\varepsilon+\beta)]^T \\
\boldsymbol{s}(m) &\triangleq [s(m) \; s(m-1) \; \ldots \; s(m-K+1)]^T \\
\boldsymbol{S}_\gamma(\varepsilon) &\triangleq [\boldsymbol{s}(\varepsilon-\gamma) \; \boldsymbol{s}(\varepsilon-\gamma+1) \; \ldots \; \boldsymbol{s}(\varepsilon+\beta)]^T
\end{aligned} \quad (4)$$

where $0 \le \gamma \le N_g - K + 1$ and $-N_g + \gamma + K - 1 \le \varepsilon \le 0$. If the training symbol is designed to have the same length as a data symbol, then $\beta + 1 = N$. The $(\gamma + \beta + 1 = N')$ length received samples vector, $\boldsymbol{r}_\gamma(\varepsilon)$, can be given by

$$\boldsymbol{r}_\gamma(\varepsilon) = e^{j2\pi\varepsilon v/N} \boldsymbol{W}_\gamma(v) \cdot \boldsymbol{S}_\gamma(\varepsilon) \cdot \boldsymbol{h} + \boldsymbol{n}_\gamma(\varepsilon) \quad (5)$$

where $\boldsymbol{W}_\gamma(v) \triangleq \boldsymbol{W}_\gamma(v,0)$. In the following, the subscript γ will be omitted for simplicity.

III. Maximum Likelihood-based Synchronization and Channel Estimation

Assume that an OFDM training symbol $\{s(k) : -N_g \leq k \leq \beta\}$ is used for timing synchronization, frequency synchronization and channel estimation. For a received observation vector $\boldsymbol{r}(\varepsilon)$ and parameters ε, v and $\boldsymbol{h}$, the likelihood function can be given by

$$\Lambda(\boldsymbol{r}(\varepsilon); \tilde{\varepsilon}, \tilde{v}, \tilde{\boldsymbol{h}}) = \frac{1}{(\pi\sigma_n^2)^{N'}} \cdot exp\{\frac{-1}{\sigma_n^2} \parallel \boldsymbol{r}(\varepsilon) - \boldsymbol{W}(\tilde{v})\boldsymbol{S}(\tilde{\varepsilon})\tilde{\boldsymbol{h}} \parallel^2\} \tag{6}$$

where $\tilde{\varepsilon}$, $\tilde{v}$, and $\tilde{\boldsymbol{h}}$ are trial values of ε, v, and $\boldsymbol{h}$ and $\| \cdot \|^2$ represents the norm-square. The conventional ML estimation of ε, v, and $\boldsymbol{h}$ can be obtained by maximizing the likelihood function (6) as follows:

$$(\hat{\varepsilon}, \hat{v}, \hat{\boldsymbol{h}})_{ML} = argmax_{\tilde{\varepsilon}, \tilde{v}, \tilde{\boldsymbol{h}}} \Lambda(\boldsymbol{r}(\varepsilon); \tilde{\varepsilon}, \tilde{v}, \tilde{\boldsymbol{h}}). \tag{7}$$

In order to define the observation vector $\boldsymbol{r}(\varepsilon)$ for the above ML estimation, a coarse timing estimation is required. At this moment, let us assume that the coarse timing estimation has been performed and the coarse timing offset is ε and the observation vector is $\boldsymbol{r}(\varepsilon)$. If $-N_g + \gamma + K - 1 \leq \varepsilon \leq 0$, the observation vector contains training signal only and the ML model (7) holds accurately. If $\varepsilon < -N_g + \gamma + K - 1$ or particularly $\varepsilon > 0$, the observation vector contains some portion of training signal and some portion of unknown data signal. Then all trial signal vectors, which are composed of training signal only, will not match the observation vector and the above ML model (7) is no longer accurate. In other words, the observation vector with $\varepsilon < -N_g + \gamma + K - 1$ or $\varepsilon > 0$ will not be a valid observation vector for the ML model (7). We will denote the ML model (7) as FOV (fixed observation vector). The coarse timing estimation may not guarantee the condition $-N_g + \gamma + K - 1 \leq \varepsilon \leq 0$. Consequently, the FOV model may no longer hold.

This leads us to another approach denoted as SOV-ML standing for the ML model with a sliding observation vector. The likelihood function for SOV-ML can be given by

$$\Lambda(\boldsymbol{r}(\tilde{\varepsilon}); \tilde{\varepsilon}, \tilde{v}, \tilde{\boldsymbol{h}}) = \frac{1}{(\pi\sigma_n^2)^{N'}} \cdot exp\{\frac{-1}{\sigma_n^2} \parallel \boldsymbol{r}(\tilde{\varepsilon}) - \boldsymbol{W}(\tilde{v})\boldsymbol{S}\tilde{\boldsymbol{h}} \parallel^2\}. \tag{8}$$

The trial signal vectors are composed of trial values $\tilde{v}$ and $\tilde{\boldsymbol{h}}$ and fixed training signal matrix corresponding to the exact timing point (i.e. $\boldsymbol{S} \triangleq \boldsymbol{S}(0)$). Note that the trial value of ε impacts on the signal model (particularly $\boldsymbol{S}(\varepsilon)$) in the likelihood function of FOV while the impact of the trial value of ε is shifted from the signal model to the received vector in SOV. The trial values of ε are embedded in sliding the observation vector within a window around the coarse timing point. In SOV, the observation vector at $\tilde{\varepsilon} = 0$ is the valid one while at other values of $\tilde{\varepsilon}$ it is not. So when the sliding window is large enough, SOV has always one valid observation vector.

Both (6) and (8) require initial coarse timing estimation. Both jointly estimate ε, v, and $\boldsymbol{h}$ to maximize the corresponding likelihood functions. This joint estimation of all parameters is associated with very high complexity. In an attempt to reduce the complexity, we resort to a sequential approach where $\tilde{\boldsymbol{h}}$ in the likelihood function is replaced by the CIR estimate $\hat{\boldsymbol{h}}$ and then ε and v are jointly estimated by maximizing the resulting likelihood function. The ML (SOV) estimates of the timing point and the normalized carrier frequency offset, denoted by ε and $\hat{v}$ respectively, are then given by

$$(\varepsilon, \hat{v})_{ML} = argmin_{\tilde{\varepsilon}, \tilde{v}} \mathcal{V}(\boldsymbol{r}(\tilde{\varepsilon}); \hat{\boldsymbol{h}}, \tilde{\varepsilon}, \tilde{v}) \tag{9}$$

where

$$\mathcal{V}(\boldsymbol{r}(\tilde{\varepsilon}); \hat{\boldsymbol{h}}, \tilde{\varepsilon}, \tilde{v}) = \boldsymbol{r}^H(\tilde{\varepsilon})\boldsymbol{r}(\tilde{\varepsilon}) - 2 \cdot \Re[\boldsymbol{r}^H(\tilde{\varepsilon})\boldsymbol{W}(\tilde{v})\boldsymbol{S}\hat{\boldsymbol{h}}] + \hat{\boldsymbol{h}}^H\boldsymbol{S}^H\boldsymbol{S}\hat{\boldsymbol{h}}. \tag{10}$$

The superscript H denotes the Hermitian transpose. Depending on the given set of parameters, the corresponding metrics to be minimized are given by

$$\mathcal{V}_{|(\hat{\boldsymbol{h}}, \tilde{\varepsilon})}(\boldsymbol{r}(\tilde{\varepsilon}); \tilde{v}) \triangleq -2 \cdot \Re[\boldsymbol{r}^H(\tilde{\varepsilon})\boldsymbol{W}(\tilde{v})\boldsymbol{S}\hat{\boldsymbol{h}}] \tag{11}$$

$$\mathcal{V}_{|\tilde{\varepsilon}}(\boldsymbol{r}(\tilde{\varepsilon}); \hat{\boldsymbol{h}}, \tilde{v}) \triangleq \mathcal{V}_{|(\hat{\boldsymbol{h}}, \tilde{\varepsilon})}(\boldsymbol{r}(\tilde{\varepsilon}); \tilde{v}) + \hat{\boldsymbol{h}}^H\boldsymbol{S}^H\boldsymbol{S}\hat{\boldsymbol{h}} \tag{12}$$

$$\mathcal{V}_{|\hat{\boldsymbol{h}}}(\boldsymbol{r}(\tilde{\varepsilon}); \tilde{\varepsilon}, \tilde{v}) \triangleq \boldsymbol{r}^H(\tilde{\varepsilon})\ \boldsymbol{r}(\tilde{\varepsilon}) + \mathcal{V}_{|(\hat{\boldsymbol{h}}, \tilde{\varepsilon})}(\boldsymbol{r}(\tilde{\varepsilon}); \tilde{v}) \tag{13}$$

$$\mathcal{V}(\boldsymbol{r}(\tilde{\varepsilon}); \hat{\boldsymbol{h}}, \tilde{\varepsilon}, \tilde{v}) = \mathcal{V}_{|\hat{\boldsymbol{h}}}(\boldsymbol{r}(\tilde{\varepsilon}); \tilde{\varepsilon}, \tilde{v}) + \hat{\boldsymbol{h}}^H\boldsymbol{S}^H\boldsymbol{S}\hat{\boldsymbol{h}}. \tag{14}$$

A. Coarse timing and frequency estimation

The first synchronization task is to detect the presence of the training symbol, especially for the burst transmission. We use a training symbol consisting of $P+1$ identical parts with M samples in each part. The first one with the time indexes $[-M, -M+1, \ldots, -1]$ can be considered as the CP. Normalized sync detection metrics give more robust sync detection performance [7]. Hence, we use the following normalized autocorrelation function as our sync detection metric:

$$\mathcal{C}(\boldsymbol{r}(k), M) \triangleq \frac{N' \left|\sum_{i=-\gamma}^{\beta-M} r^*(k+i) \cdot r(k+M+i)\right|}{(N'-M)\ \parallel \boldsymbol{r}(k) \parallel^2}. \tag{15}$$

If the metric value reaches above a threshold, the sync flag is declared. The threshold value is usually set by the missed detection and the false detection probability.

After sync detection, the coarse timing point may be taken as the sync detected point or the one that has maximum sync detection metric within a time window starting from the sync detected point. Due to the repetitive training structure, the metric $\mathcal{C}(\boldsymbol{r}(k), M)$ would give a plateau if $0 \leq \gamma < Ng - K + 1$ is used. Hence, we use $\gamma = N_g$ in (15) to avoid the metric plateau. To avoid ISI and ICI caused by positive timing offsets, the coarse timing point can be advanced by some amount λ_c (> 0). The advantage of timing advancement is discussed in [12].

For the repetitive training structure used in the sync detection, the channel output training signal still keeps the repetitive structure in the absence of noise. Consequently, the frequency offset estimation which utilizes the repetitive structure would be robust against the timing offset and the dispersive channel. Suppose the coarse timing point is within $[-M + K - 1, -M + K, \ldots, 0]$. Define a new observation variable:

$$u(k) \triangleq \sum_{p=0}^{P-2} r^*(k + p \cdot M) \cdot r(k + p \cdot M + M). \tag{16}$$

Applying MVU principle with Gaussian assumption and high SNR approximation leads to the following coarse frequency offset estimator

$$\hat{v}_c = \frac{N}{2\pi M}\ arg\{\ \sum_{k=0}^{M-1} u(k)\ \} \tag{17}$$

where the estimation range is $-\frac{N}{2\ M} < \hat{v}_c \leq \frac{N}{2\ M}$.

B. Fine timing and frequency estimation

The ML estimates $(\varepsilon, \hat{v})_{|(\varepsilon_c, \hat{v}_c)}$ which is based on the coarse estimates $(\varepsilon_c, \hat{v}_c)$ can be obtained from (9) as

$$(\varepsilon, \hat{v})_{|(\varepsilon_c, \hat{v}_c)} = argmin_{(\tilde{\varepsilon}, \tilde{v})}\{\mathcal{V}(\boldsymbol{r}(\tilde{\varepsilon}); \hat{\boldsymbol{h}}, \tilde{\varepsilon}, \tilde{v}) : \\ \varepsilon_c - T_1 \le \tilde{\varepsilon} \le \varepsilon_c + T_2,\ \hat{v}_c - F_1 \le \tilde{v} \le \hat{v}_c + F_2\}. \quad (18)$$

Equation (18) can be implemented by first finding $\tilde{v}$ that minimizes the metric for each $\tilde{\varepsilon}$, denoted by $\hat{v}_{|\tilde{\varepsilon}}$, and then choosing the pair $(\tilde{\varepsilon}, \hat{v}_{|\tilde{\varepsilon}})$ that has minimum metric, denoted by $\mathcal{V}_{(\varepsilon_c, \hat{v}_c)}$. By using (11), an ML estimate of v for a trial timing point $\tilde{\varepsilon}$ is obtained as

$$\hat{v}_{|\tilde{\varepsilon}} = argmin_{\tilde{v}}\{\mathcal{V}_{|(\hat{\boldsymbol{h}}, \tilde{\varepsilon})}(\boldsymbol{r}(\tilde{\varepsilon}); \tilde{v}) \ : \hat{v}_c - F_1 \le \tilde{v} \le \hat{v}_c + F_2\} \quad (19)$$

with the corresponding minimum metric $\mathcal{V}_{|(\hat{\boldsymbol{h}}, \tilde{\varepsilon})}(\boldsymbol{r}(\tilde{\varepsilon}); \hat{v}_{|\tilde{\varepsilon}})$. Then, by using (13), an ML timing estimate is obtained as

$$\varepsilon_f = argmin_{\tilde{\varepsilon}}\{\mathcal{V}_{|\hat{\boldsymbol{h}}}(\boldsymbol{r}(\tilde{\varepsilon}); \tilde{\varepsilon}, \hat{v}_{|\tilde{\varepsilon}}) \ : \varepsilon_c - T_1 \le \tilde{\varepsilon} \le \varepsilon_c + T_2\} \quad (20)$$

and the fine estimates are given by $(\varepsilon_f, \hat{v}_f)$ with $\hat{v}_f = \hat{v}_{|\varepsilon_f}$.

The realization of (18) requires the knowledge of CIR which is not affected by the (coarse) timing and frequency offsets. [12] presents a method to estimate the required CIR for (18). Let this CIR estimate based on the $(\varepsilon_c,\ \hat{v})$ be $\hat{\boldsymbol{h}}(\varepsilon_c, \hat{v}_c)$. This estimate is valid if the coarse timing offset is within the range $-K_4 \le \varepsilon_c \le K_3$ where $K_3 + K_4 + 1 = M$. To extend the coarse timing offset range for which the CIR estimation works, we consider three candidates of coarse timing offset, namely $\{\varepsilon_i \ : i = -1, 0, 1\}$ with $\varepsilon_i = \varepsilon_c + i \cdot M$. For each set $(\varepsilon_i, \hat{v}_c)$, realizing (18) results in a candidate set of fine estimates $(\varepsilon_f, \hat{v}_f)_i$ together with the corresponding minimum metric $\mathcal{V}_{(\varepsilon_i, \hat{v}_c)}$. The fine estimates are then obtained as

$$(\varepsilon_f, \hat{v}_f) = argmin_{(\varepsilon_f, \hat{v}_f)_i}\{\mathcal{V}_{(\varepsilon_i, \hat{v}_c)} : i = -1, 0, 1\}. \quad (21)$$

The allowable coarse timing offset range is now extended to $-M - K_4 \le \varepsilon \le M + K_3$ which is usually more than sufficient for the SNR of interest.

After obtaining ε_f and $\hat{v}_f$, fine estimation stage can be iterated for further improvement. At this time, ambiguity resolution will no longer be required, i.e., no need to consider three candidate sets. The final estimates can be taken from the last iteration or from the iteration with minimum metric.

1) Implementation of fine frequency estimation: Define $\hat{\boldsymbol{r}}_{ref} \triangleq \boldsymbol{S}\hat{\boldsymbol{h}}$ whose elements are $\{\hat{r}_{ref}(k)\}$, where $\hat{\boldsymbol{h}}$ is obtained from [12] used in the chosen set among $\{\varepsilon_i, \hat{v}_c\}$ (or, if at further iteration of the fine synchronization, it is obtained from [12] with previous ε_f and $\hat{v}_f$). Then, (11) can be realized as

$$\mathcal{V}_{|(\hat{\boldsymbol{h}}, \tilde{\varepsilon})}(\boldsymbol{r}(\tilde{\varepsilon}); \tilde{v}) = -2 \cdot Re[\sum_{k=-\gamma}^{\beta} q(k)\ e^{-j2\pi\tilde{v}k/N}] \quad (22)$$

where $q(k) \triangleq \hat{r}^*_{ref}(k)\ r(\tilde{\varepsilon} + k)$. After obtaining $\{q(k)\}$ for a trial point $\tilde{\varepsilon}$, (19) can be implemented in an iterative way using (22) as follows: Set $F_1 = F_2;\ \hat{v}_0 = \hat{v}_c;\ \Delta_0 = F_1/J_1$

for $i = 1 : 1 : J_2$
$\quad \tilde{v}_k = \hat{v}_{i-1} + k \cdot \Delta_{i-1}$
$\quad \hat{v}_i = argmin_{\tilde{v}_k}\{\mathcal{V}_{|(\hat{\boldsymbol{h}}, \tilde{\varepsilon})}(\boldsymbol{r}(\tilde{\varepsilon}); \tilde{v}_k) \ : k = -J_1 : 1 : J_1\}$
$\quad \Delta_i = \xi \cdot \Delta_{i-1}/J_1$
end
$\hat{v}_{|\tilde{\varepsilon}} = \hat{v}_{J_2}.$ (23)

Depending on the coarse frequency estimation performance, the value of F_1 can appropriately be set for complexity reduction. The parameters (J_1, J_2, ξ) give a trade-off between accuracy and complexity. Alternatively, (19) can be implemented by FFT and interpolation as in [11].

C. Estimation of channel frequency response

The fine timing point will be most of the time at the correct point and hence, the channel estimation performed then can be based on the $(\beta + N_g - K + 2)$ length received vector $\boldsymbol{r}$, (i.e., with $\gamma = N_g - K + 1$), as follows:

$$\hat{\boldsymbol{h}}_f = (\boldsymbol{S}^H_\gamma \boldsymbol{S}_\gamma)^{-1} \boldsymbol{S}^H_\gamma \boldsymbol{W}^H_\gamma(\hat{v}_f) \boldsymbol{r}_\gamma(\varepsilon_f). \quad (24)$$

If we have knowledge of the number of nontrivial channel taps $\mathcal{K}$, the channel estimation can further be improved by using the $\mathcal{K}$ largest energy taps out of K estimated taps [9]. To account for the occasional occurrence of $\varepsilon_f > 0$ which will cause ISI, the fine timing estimate is advanced by some amount λ_f (> 0). In this case, $\hat{\boldsymbol{h}}_f$ which is obtained above with no timing advancement can be modified as

$$\hat{\boldsymbol{h}}_f(\lambda_f) = e^{-j2\pi\hat{v}_f\lambda_f/N}\ [\boldsymbol{0}_{1\times\lambda_f},\ \hat{\boldsymbol{h}}^T_f]^T. \quad (25)$$

Finally, N point FFT of $\hat{\boldsymbol{h}}_f(\lambda_f)$ gives the sub-channel frequency response estimates.

IV. Performance Analysis

Let $\Delta\boldsymbol{h} = \hat{\boldsymbol{h}} - \boldsymbol{h}$ and $\boldsymbol{C}_{\Delta\boldsymbol{h}} = E[\Delta\boldsymbol{h}\Delta\boldsymbol{h}^H]$. Following the method from [11] and assuming that $E[\Delta h(k)] = 0$, we obtain $E[\hat{v}] = v$ and

$$var[\hat{v}] \simeq \frac{\boldsymbol{s}^H\ \boldsymbol{s}}{2N\ \text{SNR}\ (\boldsymbol{y}^H\ \boldsymbol{y})} \\ +\ \frac{\boldsymbol{y}^H\boldsymbol{S}\boldsymbol{C}_{\Delta\boldsymbol{h}}\boldsymbol{S}^H\boldsymbol{y} + \frac{4\pi^2}{N^2}\ \frac{\boldsymbol{s}^H\ \boldsymbol{s}}{N\ \text{SNR}}\ tr\{\boldsymbol{\mathcal{W}}\boldsymbol{S}\boldsymbol{C}_{\Delta\boldsymbol{h}}\boldsymbol{S}^H\boldsymbol{\mathcal{W}}\}}{2(\boldsymbol{y}^H\boldsymbol{y})^2} \quad (26)$$

where $\boldsymbol{y} \triangleq \frac{2\pi}{N}\ \boldsymbol{\mathcal{W}}\boldsymbol{S}\boldsymbol{h}$, $\boldsymbol{\mathcal{W}} \triangleq diag\{-N_g\text{+}K - 1,\ -N_g\text{+}K,\ \ldots,\ \beta\}$, and $\boldsymbol{s} \triangleq [s(0), s(1), \ldots, s(N-1)]^T$. Equation (26) indicates that the frequency estimation accuracy depends on the channel response, the training symbol and the channel estimation error.

Similarly, the channel estimation MSE, for a particular $\Delta v \triangleq \hat{v} - v$ and $\boldsymbol{h}$, can be given by

$$\text{MSE}[\hat{h}(k)] \ \simeq\ \left[\frac{\boldsymbol{s}^H\boldsymbol{s}\ (\boldsymbol{S}^H\boldsymbol{S})^{-1}}{N\ \text{SNR}} + \{\boldsymbol{I} - \boldsymbol{S}^H\boldsymbol{W}(\Delta v)\boldsymbol{S}(\boldsymbol{S}^H\boldsymbol{S})^{-1}\}\right. \\ \cdot\ \left.\{\boldsymbol{h}\boldsymbol{h}^H - (\boldsymbol{S}^H\boldsymbol{S})^{-1}\boldsymbol{S}^H\boldsymbol{W}^H(\Delta v)\ \boldsymbol{S}\boldsymbol{h}\boldsymbol{h}^H\}\right]_{k,k} \quad (27)$$

Equation (27) indicates that the channel estimation accuracy depends on the frequency estimation accuracy.

V. Simulation Results and Discussions

OFDM system parameters are $N = 64$, 52 used sub-carriers, $N_g = 16$, and QPSK modulation. The training symbol is composed of $P + 1 = 5$ identical parts and each part is generated by 16 point IFFT of length-16 Golay complementary sequence. The channel path gains $\{h_l; l = 0,\ 1,\ \ldots, 7\}$ are WSSUS complex Gaussian with sample-spaced path delays and $K = 8$, $t_0 = 0$. The channel power delay profile is with a -3 dB per tap decaying factor. Other parameters are $\lambda_c = 4$, $\lambda_f = 2$, $v = 1.6$, $F_1 = 0.1$, $J_1 = 10$, $J_2 = 5$, $\xi = 2$, $T_1 = K_3 = 4$, $T_2 = K_4 = 11$, $K' = K = 8$ and

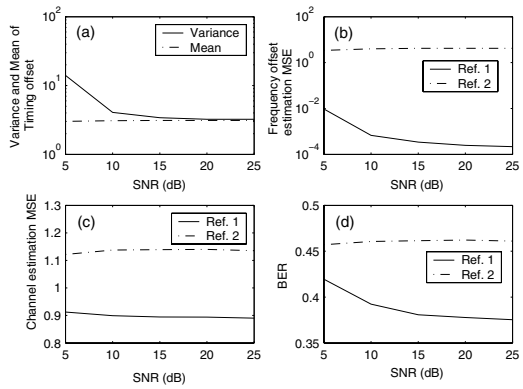

Fig. 1. The performances of the reference schemes

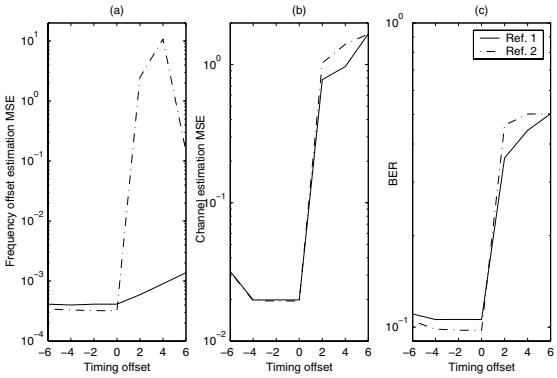

Fig. 2. The performances of the reference schemes at different fixed timing offsets and SNR value of 10 dB

$\mathcal{K} = 8$ unless stated otherwise. One packet is composed of one training symbol and 5 data symbols and the results are obtained from 10^5 simulation runs.

As an illustration of the impacts of errors from one of the tasks of synchronization and channel estimation on the others, two reference schemes are evaluated. The first reference scheme consists of the timing offset estimation from [6] with 90% maximum point averaging, the frequency offset estimation from [4] and the ML-based channel estimation used in [11](same as (24) with $\gamma = 0$). The second reference scheme consists of the timing offset estimation from [6] with 90% maximum point averaging, the MLE#2 frequency offset estimation from [4] and the channel estimation used in [11]. In MLE#2 frequency offset estimation, an FFT pruning factor of 4 is used and a quadratic interpolation is performed to get a fine frequency offset estimate. Fig. 1 presents the performances of the two reference schemes. Fig. 1(a) indicates that the timing offset estimation would definitely introduce ISI and ICI since the mean of timing offset is greater than zero. Fig. 1(b) shows that the frequency offset estimator MLE#2 (Ref. 2) fails to give reliable estimate. Fig. 1(c)(d) indicate that both reference schemes fail. The reason is better explained in Fig. 2 where the frequency offset estimation, the channel estimation and the BER performances of both reference schemes are presented for different fixed timing offset values at SNR = 10 dB. The results show that errors in one task can affect the other tasks in synchronization and channel estimation and this fact should be taken into consideration in the design/derivation of the synchronization and channel estimation methods.

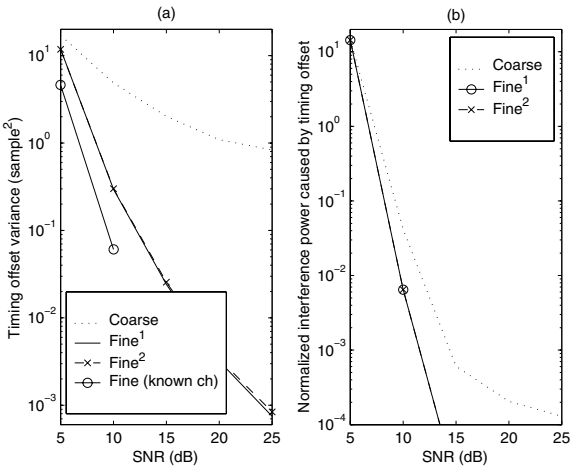

Fig. 3. Timing offset estimation performance

Fig. 3 (a) presents the timing offset variances where "Fine^k" denotes the k^{th} iteration at the fine synchronization stage. The estimation performance is much improved in the fine stage but more iteration does not improve timing estimation further. Fig. 3 (a) also includes the performance with known CIR. The corresponding variance for SNR of 15 dB and above are not present for no timing offset is observed in the simulation. The average normalized interference power caused by the timing estimation (calculated as in [7]) is presented in Fig. 3 (b). Same trend as in the variance performance is observed.

Fig. 4(a) shows the frequency offset estimation MSE performance. More iteration of the fine synchronization improves the frequency estimation performance although it does not improve the timing estimation. Hence, if more than one iteration is used, the fine timing estimation part can be skipped after the first iteration. We have also evaluated the performance of the fine frequency estimation with [4] as a coarse estimation, and a slight improvement is observed. The result denoted by "Fine (selected)" is obtained from the iteration with the minimum metric among the 5 iterations. It has a slight improvement over "Fine^5" case. The performance of the fine frequency estimation with known CIR is also included as a lower bound. The performance gap can be viewed as the sensitivity of the fine synchronization to the channel estimation errors. Fig. 4(a) also includes the Cramer-Rao bound in AWGN channel (CRB_1) and the CRB in AWGN channel with perfect phase synchronization (CRB_2). Fig. 4(b) presents the channel estimation MSE performance. In the case of the coarse synchronization only, in order to account for some timing offsets and not to miss some channel taps, $K' = N_g$ is used. Clearly, all cases of the fine stage have much better performance than the coarse synchronization only case. More iterations at the fine stage have slightly improved channel estimation and "Fine(selected)" case has the best performance.

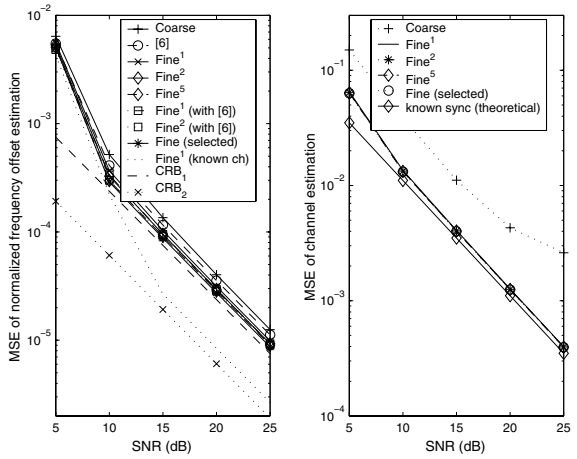

Fig. 4. (a) The normalized frequency offset estimation performance (b) The channel estimation performance

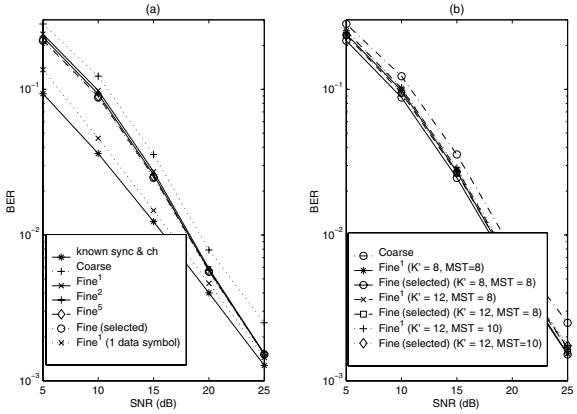

Fig. 5. BER performance of the proposed method with: (a) Matched parameters (b) Mismatched parameters

The channel estimation performance of the proposed method is quite close to the theoretical performance obtained with known sync parameters.

In Fig. 5(a), BER performance curves are presented. The fine stages have better BER than the coarse stage due to better synchronization and channel estimation. More iteration in the fine stage slightly improves the BER especially at moderate and low SNR values. "Fine (selected)" case has a marginally better BER than other cases. The BER of the proposed approach for a packet containing one training symbol and one data symbol is also listed. It reflects more about the snap-shot synchronization and channel estimation errors effect. The results indicate that the proposed scheme performance is quite close to the performance with known sync parameters and known channel response. We have evaluated the proposed method with the designed maximum channel delay spread K' and the designed number of the most significant channel taps $\mathcal{K}$ (which is denoted by "MST" in the figure) different from their actual values. The BER curves are given in Fig. 5(b). Due to the noise contamination from the extra taps, a slight performance loss is observed. However, considerable performance improvement over the coarse stage is still achieved. We have also evaluated the proposed approach in the HiperLAN channel model-A (non-sample-spaced path delays). The results show the same trend and hence, are omitted.

VI. Conclusions

In synchronization and channel estimation tasks, errors from one task can affect the other tasks. Separately addressing each individual task may not reflect actual performance. This has motivated the development of the proposed combined approach for synchronization and channel estimation tasks. The proposed approach consists of two stages. At the first stage, robust sync detection and simple coarse synchronization tasks are accomplished by using the repetitive structure of the training symbol. At the second stage, an ML estimation of timing and frequency offsets based on sliding observation vector (SOV) is realized by using the coarse estimates of the sync parameters and the CIR. Then ML channel estimation is performed. The simulation results show that the proposed combined approach performs quite well and circumvents the problem of high sensitivity of one task to errors in other tasks.

Acknowledgment

This work was supported in part by the School of Engineering and Computer Science at the University of Texas at Dallas and in part by the Natural Sciences and Engineering Research Council (NSERC) of Canada.

References

[1] D. Landström, S. K. Wilson, J.J. van de Beek, P. Ödling and P. O. Börjesson, "Symbol time offset estimation in coherent OFDM systems," *IEEE Trans. Commun.*, Vol. 50, Issue 4, pp. 545-549, Apr. 2002.

[2] B. Yang, K. B. Letaief, R. S. Cheng and Z. Cao, "Timing recovery for OFDM transmission," *IEEE J. Select. Areas in Commun.,* Vol. 18, No. 11, pp. 2278-2290, Nov. 2000.

[3] P.H. Moose, "A technique for orthogonal frequency division multiplexing frequency offset correction," *IEEE Trans. on Commun.*, Vol. 42, No. 10, pp. 2908-2914, Oct 1994.

[4] M. Morelli and U. Mengali, "An improved frequency offset estimator for OFDM applications," *IEEE Commun. Letters*, Vol. 3, No. 3, Mar 1999, pp. 75-77.

[5] J-J. van de Beek, M. Sandell and P.O. Börjesson, "ML estimation of time and frequency offset in OFDM systems" *IEEE Trans. Signal Proc.*, Vol. 45, no. 7, July 1997, pp. 1800-1805.

[6] T. M. Schmidl and D. C. Cox, "Robust frequency and timing synchronization for OFDM," *IEEE Trans. Commun.*, Vol. 45, No. 12, Dec 1997, pp. 1613-1621.

[7] H. Minn, V. K. Bhargava and K. Ben Letaief, "A robust timing and frequency synchronization for OFDM systems," *IEEE Trans. Wireless Commun.*, Vol. 2, No. 4, pp. 822-839, July 2003.

[8] O. Edfors, M. Sandell, J.-J. van de Beek, S. K. Wilson and P. O. Borjesson, "OFDM channel estimation by singular value decomposition," *IEEE Trans. Commun.* vol. 46, pp. 931-939, Jul 1998.

[9] Y. Li, L. J. Cimini, Jr., and N. R. Sollenberger, "Robust channel estimation for OFDM systems with rapid dispersive fading channels," *IEEE Trans. Commun.*, vol. 46, pp.902-915, Jul 1998.

[10] M. Speth, S. A. Fechtel, G. Fock and H. Meyr, "Optimum receiver design for wireless broad-band systems using OFDM-Part I," *IEEE Trans. Commun.*, Vol. 47, No. 11, Nov. 1999, pp. 1668-1677.

[11] M. Morelli and U. Mengalli, "Carrier-frequency estimation for transmissions over selective channels," *IEEE Trans. Commun.*, Vol. 48, No. 9, Sept. 2000, pp. 1580-1589.

[12] H. Minn, V.K. Bhargava and K. Ben Letaief, "Channel estimation assisted improved timing offset estimation," *accepted in IEEE ICC 2004, Communications Theory Symposium.*